NUMERICAL AND EXPERIMENTAL ANALYSES OF PIEZOELECTRIC FANS FOR MICROELECTRONICS COOLING

MARAM VENKATA RAMANA

UNIVERSITI SAINS MALAYSIA

2010

NUMERICAL AND EXPERIMENTAL ANALYSES OF PIEZOELECTRIC FANS FOR MICROELECTRONICS COOLING

by

MARAM VEKATA RAMANA

Thesis submitted in fulfillment of the requirements

for the degree of

Doctor of Philosophy

June 2010

ACKNOWLEDGEMENTS

It is my great pleasure to express my sincere and heartfelt gratitude to my research supervisors Assoc. Prof. Dr. Indra Putra Almana and Assoc. Prof. Dr. Zulkifly Abdulla for their guidance, support, and friendly nature in carrying out this research work. Special thanks go to them for their patience on me during the course. It was a great experience to work with them. I also learnt many things by closely observing them.

I would like thank the Dean, School of Mechanical Engineering for accepting me into the doctoral research program and for providing necessary facilities to carry out this research work. Thanks also to the staff of the school for their prompt help.

I would like to thank my earlier supervisor Prof.K.N.Seetharamu for his technical guidance and moral support during the course of this research program.

I owe my deepest gratitude to Prof. Aswatha, as nothing would have been possible without his beneficial directions and essential push from the beginning to the final level of this dissertation. I extend my appreciation to Mrs.Shantha Narayana for her personal care.

Thanks are due to my fellow friends Irfan, Jeevan, Kulakarni, Khalid, Lee Kor Onn and Varadharaju for their help and moral support. Special thanks to my friends

Salman and Zubhair for their help during compiling this work and their gesture. I am also thankful to all those who have helped and supported me directly or indirectly during the course of this program.

I dedicate this work to my wife M Sandhya Rani for her continuous encouragement and unconditional sacrifices. I thank my parents and in-laws for their extended support on raising my kids.

Last but not least, I would like to express my appreciation to my friend Mr.Vasu and Mrs.Vasu for providing accommodation while compiling this work.

Maram Venkata Ramana

JUNE, 2010.

TABLE OF CONTENTS

	Page
ACKNOWLEDGEMENTS	i
TABLE OF CONTENTS	iii
LIST OF TABLES	viii
LIST OF FIGURES	ix
LIST OF ABBREVIATION	xiii
ABSTRAK	xvii
ABSTRACT	xix

CHAPTER ONE: INTRODUCTION

1.1	Thermal management of electronic systems	1
1.1.1	Background	1
1.1.2	Natural Cooling	4
1.1.3	Forced Air Cooling	4
1.1.4	Forced Liquid Cooling	5
1.1.5	Micro-channel heat exchanger	6
1.1.6	Heat Conduction via Embedded Solids	7
1.1.7	Miniaturized Vapor absorption refrigeration	7
1.1.8	Use of heat pipes as heat sinks	8
1.1.9	Impingement or Spray cooling	9
1.1.10	Hybrid Air-water Cooling	9

1.2 Piezo-Electric Fan for Micro-Electronic Cooling 10
1.2.1 Introduction 10
1.2.2 Piezoelectricity and its Evolution 11
1.2.3 Piezoelectric Materials 14
1.2.4 Piezoelectric Actuators 16
1.2.5 Stacks 16
1.2.6 Unimorph 17
1.3 Problem Statement 24
1.4 Research Objectives 26
1.5 Scope of the Current Research 27
1.6 Thesis outline 28

CHAPTER TWO: LITERATURE REVIEW

2.0 Introduction 29
2.1 Piezoelectricity 30
2.2 Piezoelectric fans for electronic cooling 31
2.2.1 Numerical and experimental investigation of piezoelectric fan 33
2.2.2 Artificial Numerical Technique ANN prediction 35
2.2.3 Flow visualization method analysis of piezofan 40
2.2.4 Performance and optimization of the piezo fan 41
2.3 Particle image velocimetry (PIV): Flow visualization technique 45
2.4 Critical Literature review 53

CHAPTER THREE: METHODOLOGY

3.1	Numerical Simulation of Piezoceramic Bimorph Beam	55
	3.1.1 Introduction	55
	3.1.2 Numerical Simulation Method	56
	3.1.3 Finite Element Analysis	57
	3.1.4 ANSYS	58
	3.1.5 Coupled Field Analysis	59
	3.1.6 Piezoelectric Finite Element Formulation	60
	3.1.7 Finite Element Discretization Equation	66
	3.1.8 Piezoelectric Analysis	69
3.2	Genetic Algorithms(GA)	73
	3.2.1 Neuro-Genetic approach	76
3.3	Numerical Modeling and simulation	77
	3.3.1 Modeling	77
	3.3.2 The physical model for Horizontal piezofan	79
3.3.3	Modeling	80
3.3.3	Model Creation	82
3.3.4	Grid Generation	83
3.3.5	The physical model for Vertical piezofan	84
3.3.6	2D CFD Modeling	85
3.4	PIV-experimental setup and analysis	89
3.4.1	Introduction	89

3.4.2 Components of PIV 90

3.4.2.1 Seeding Particle 90

3.4.2.2 CCD Camera 91

3.4.2.3 Illumination 92

3.4.2.4 Experimental Apparatus 92

3.4.2.5 Experimental Uncertainty Measurement 95

CHAPTER FOUR: RESULTS AND ANALYSES OF NUMERICAL SIMULATION

4.1 Introduction 96

4.2 Design and optimization of the piezoelectric fan 97

4.2.1 Effect of thickness ratio (B) on tip-deflection (δ) 98

4.2.2 Effect of thickness ratio (B) on resonance frequency (f) 99

4.2.3 Effect of damping ratio 100

4.2.4 Effect of bimorph length 101

4.2.5 Effect of temperature on tip-deflection 103

4.2.6 Effect of temperature on first ultrasonic resonance frequency 104

4.2.7 Effect of applied electric field 105

4.2.8 Effect of Width, *w* 106

4.2.9 Discrete Piezoelectric Actuators that Occupy a Small Area of the Structure 107

4.2.10 Effect of *LP/L* Ratio to Four Models of Discrete Piezoelectric Structure 108

4.2.11 Optimization of Piezoelectric Structure Design 115

4.3 Application of ANN and GA 119

4.4 Numerical Simulation using Fluent 121

4.4.1 Characteristic Surface Velocity 122

4.4.2 Effect of Gap on Chip Temperature 126

4.4.3 Heat Transfer Coefficient Variation 129

4.4.4 Effect of piezoelectric fan Height on flow and heat transfer for microelectronic cooling applications 133

4.5 PIV Results and discussion 141

4.5.2 Effect of fan location on the flow orientation 141

4.5.3 Schematic diagram of the different case set up 142

4.5.4 Vector Plot comparison for different cases 157

4.5.5 Streamlines comparison 160

4.5.6 Validation of the CFD results with the PIV experimental results 163

CHAPTER FIVE: CONCLUSIONS AND RECOMMENDATIONS

5.1 Conclusions 168

5.2 Scope of Future Work 170

REFERENCES 170

LIST OF PUBLICATIONS 179

APENDICES 181

LIST OF TABLES

Page

4.1 Material properties of PSI-5H at room temperature 96

4.2 bimorph length increases its fundamental resonance frequency 98

4.3 Surface velocities for different bimorph lengths 99

4.4 Material Properties 112

4.5 Bimorph configurations 113

4.6 Case 1 Comparative performance merit 115

4.7 Optimum values from genetic Algorithm 116

4.8 Comparison of results from the published and present work 118

4.9 Comparative air velocities produced by five bimorph configurations 120

4.10 List of simulated chip temperature from the analysis 124

4.11 Average surface heat transfer coefficients 128

5.1 Description of different cases 144

LIST OF FIGURES

Page

1.1 Major causes of electronic failures 3
1.2 Schematic diagram of a forced liquid convection cooling system 5
1.3 Schematic representation of a micro channel heat exchanger 6
1.4 Schematic diagram of an absorption based heat pump system 8
1.5 Various configurations of round and slot jets, singly and in arrays 9
1.6 Schematic and picture of a piezo fan. 11
1.7 Piezoelectric material changes according to the electric field and polarization direction 12
1.8 Diagram of piezoelectric stack 17
1.9 A RAINBOW stack actuator 18
1.10 Layers in a THUNDER actuator 19
1.11 Structure of cantilever bimorph 21
1.12 Chronological Variation in chip density of microprocessor 22
1.13 Moore's law showing the increase in circuit complexity over time 22
3.1 Peizoceramic Bimorph 74
3.2 Single blade 75
3.3 Two blades 76
3.4 Three blades 76
3.5 Four blades 76
3.6 Five blades 77
3.7 Flow chart of Neuro-genetic optimization 80
3.8 Isometric view of the flow domain for the case 2 85
3.9 The grid of the flow domain considered for the CFD simulation 87
3.10 2D domain description of the CFD domain 90
3.11 The CFD grid 90
3.12 2D view of the meshed flow domain for the CFD simulation 91
4.1 Structure of Piezoelectric Bimorph 93

4.2	Static Tip Deflection Vs Thickness Ratio	94
4.3	Resonance Frequency Vs Thickness Ratio	95
4.4	Harmonic response for different damping ratios	97
4.5	Temperature dependent material properties for PSI-5H and PSI-5A	99
4.6	Tip-deflection observed at different temperatures	100
4.7	First ultrasonic resonance frequency Vs Temperature	101
4.8a	Static tip-deflection Vs Electric field applied	102
4.9	The first ultrasonic resonance frequency versus width of a bimorph	103
4.10	Four models of the discrete piezoelectric structure	105
4.11	Dimension of the model 3	106
4.12	Different mode shapes of the piezoelectric fans	107
4.13	The performance merit versus LP/L ratio for model 1	108
4.14	The performance merit versus LP/L ratio for model 2	108
4.15	The performance merit versus LP/L ratio for model 3	109
4.16	The performance merit versus LP/L ratio for model 4	110
4.17	Schematic piezoelectric bimorph model	113
4.18	Amplitude of bimorph, L =0.6cm	113
4.19	Amplitude of bimorph, L =0.8cm	114
4.20	Amplitude of bimorph, L =1.0cm	114
4.21	Case2 ANN predictions with ANSYS input data	116
4.22	Case 3 ANN predictions with ANSYS input data	117
4.23	First ultrasonic resonance frequency of bimorph with two blades	121
4.24	Dynamic tip-deflection of bimorph with three blades	121
4.25	Contours of static temperature for the model 3 when gap 10mm and power 0.25W	122
4.26	Front surface heat transfer coefficient distribution when gap 20 mm and chip power 0.5W	126
4.27	Front surface heat transfer coefficient distribution when gap = 20 mm and chip power = 0.5W	127
4.28	Contours of surface heat transfer coefficient for case 5 when gap 20mm and power 0.5W	127

4.29	Contents of surface heat transfer coefficient for case 4 when gap 20mm and power 0.5W	128
4.30	Velocity vectors for Case A ($h/l_P = 0.13$) induced by the piezofan	129
4.31	Velocity vectors for Case B ($h/l_P = 0.23$) induced by the piezofan	130
4.32	(a)-(d) Velocity magnitude for Case A at different time interval	131
4.33	(a)-(d) Velocity magnitude for Case B at different time interval	133
4.34	(a)-(d) Temperature contours for Case A at different time interval	134
4.35	(a)-(d) Temperature contours for Case B at different time interval	136
5.1	The experimental setup	141
5.2	Piezo-fan with two heat source arrangement	142
5.3	Particle Image Velocimetry (PIV) with Piezo-Fan and Heat Source Arrangement	142
5.4	Schematic diagrams of different case set ups	145
5.5	The schematic figure showing the left swing of the fan	146
5.6	The vector diagram showing the orientation of the fluid due to left swing of the fan	146
5.7	The stream lines figures showing the flow characteristics	147
5.8	V-velocity component at 5.5mm and 10mm left of the fan when fan swings left	148
5.9	The V-velocity at the left of the piezofan due to the right ward swing of the fan	148
5.10	V-Velocity component at 6mm,12mm and 14mm from the heater surface	150
5.11	The schematic figure of the piezofan set up exhibiting right swing	151
5.12	The vector diagram showing the orientation of the fluid due to right swing of the fan	152
5.13	The stream lines figures showing the flow characteristics when fan swing rightward	152
5.14	V-velocity component at 5.5mm and 10mm left of the fan when fan swings right	153
5.15	V-Velocity component at 6mm,12mm and 14mm from the heater surface	155
5.17	Comparison of the fluid flow between left and right swing of the fan at 6mm height from the heater surface	155

5.18	Comparison of the fluid flow between left and right swing of the fan at 12mm height from the heater surface	156
5.19	Comparison of the fluid flow between left and right swing of the fan at 14mm height from the heater surface	156
5.20	Comparison of the fluid flow made at 5.5mm left of the piezofan between left and right swing of the fan at 14mm height from the heater surface	157
5.21	Comparison of the fluid flow (made at 10mm left of the piezofan) between left and right swing of the fan at 14mm height from the heater surface	158
5.22	Comparison of the fluid flow (made at 5.5mm right of the piezofan) between left and right swing of the fan at 14mm height from the heater surface	158
5.23	Comparison of the fluid flow (made at 10mm left of the piezofan) between left and right swing of the fan at 14mm height from the heater surface	159
5.24	Case A: Vector plot for left swing	160
5.25	Case B: Vector plot for left swing	161
5.26	Case C: Vector plot for left swing	161
5.27	Case A: Streamlines for left wing	162
5.28	Case B: Streamlines for left wing	162
5.29	Case C: Streamlines for left wing	163
5.30	Comparison of the PIV and CFD vector plots	164
5.31	Comparison of the PIV and CFD U velocity	165
5.32	Comparison of the PIV and CFD stream lines	165
5.33	Experimental heat transfer coefficient for different cases	166
5.34	Validation of the PIV and CFD heat transfer coefficient	167

LIST OF ABBREVIATIONS

A	Young's modulus of metal to Young's modulus of piezoelectric material ratio $\frac{E_m}{E_p}$
B	Thickness of metal layer to total thickness of piezo layers ratio $\frac{t_m}{2t_p}$
C	Density of metal to density of piezoelectric material ratio $\frac{\rho_m}{\rho_p}$
C_k	Element damping matrix
C_ξ	Frequency-dependent damping matrix
c_{ij}	Stiffnesses with respect to the i, j-directions
D	Dynamic tip deflection
d_{31}	Piezoelectric constant
E_3	Electric field strength applied to the piezoelectric layers
E_{ij}	Young's modulus in the ith-direction
E_m	Young's modulus of metal
E_p	Young's modulus of piezoelectric layers
E^{po}	Potential energy
f_1	Fundamental resonance frequency
f_r	Resonance frequency

G_{ij}	Shear modulus with respect to the *i*, *j*-directions
K_j	Portion of structure stiffness matrix based on material j
L	Length of the piezoelectric structure
LP	Total length of piezo actuator at the discrete piezoelectric structure
N_i	Shape function for node i
NEL	Number of element with specified damping
$NMAT$	Number of materials with DAMP input
n	Number of nodes of the element
s_{ij}	Compliances with respect to the *i*, *j*-directions
T	Total thickness of the piezoelectric structure
t_m	Thickness of metal layer
t_p	Thickness of each piezoelectric layer
U_D	Dielectric Energy
U_E	Elastic Energy
U_M	Electromechanical Coupling Energy
V_c	Electrical potential within element domain
v	Characteristic surface velocity of the flexural vibrating cantilever bimorph
v_{ij}	Poisson's ratio reflecting the contraction in the *j*th-direction with respect to the *i*-directions
w	Width of piezoelectric structure
α	Constant mass matrix multiplier

β	Constant stiffness matrix multiplier
β_c	Variable stiffness matrix multiplier
β_j	Constant stiffness matrix multiplier for material j
δ	Static tip deflection
λ_r	Roots of the solution for the resonance frequency expression
ρ	Mass density
ρ_m	Density of metal
ρ_p	Density of piezoelectric layers
$[B_u]$	Derivative matrix of shape function matrix $[N^u]$
$[B_V]$	Derivative matrix of shape function matrix $[N^V]$
$[C]$	Structural damping matrix
$[c]$	Elasticity/stiffness matrix (evaluated at constant electric field)
$\{D\}$	Electric flux density vector
$[d]$	Piezoelectric strain matrix
$\{E\}$	Electric field vector
$[e]$	Piezoelectric stress matrix
$\{F\}$	Vector of nodal forces, surface forces and body forces
$\{F^{ac}\}$	Force vector due to acceleration effects
$\{F^{nd}\}$	Applied nodal force vector

$\{F^{pr}\}$	Pressure load vector
$\{F^{th}\}$	Thermal strain force vector
$[K]$	Structural stiffness matrix
$[K^{d}]$	Dielectric conductivity matrix
$[K^{Z}]$	Piezoelectric coupling matrix
$\{L\}$	Applied nodal charge vector
$\{L^{nd}\}$	Applied nodal charge vector
$[M]$	Structural mass matrix
$[N^{u}]$	Matrix of displacement shape functions
$\{N^{V}\}$	Vector of electrical potential shape function
$\{S\}$	Strain vector
$[s]$	Compliance matrix
$\{T\}$	Stress vector
$\{u\}$	Vector of nodal displacements
$\{u_{c}\}$	Displacement within element domain in the X, Y, Z directions
$\{V\}$	Vector of nodal electrical potential
$[\varepsilon]$	Permittivity/dielectric matrix (evaluated at constant mechanical strain)

ANALISA BERANGKA DAN EKSPERIMEN KIPAS PIEZOELEKTRIK BAGI PENYEJUKAN MIKROELEKTRONIK

ABSTRAK

Dalam kemajuan sains dan teknologi, produk elektronik bergerak maju dan mempunyai banyak fungsi. Produk elektronik juga telah mengecil saiz dan berat yang mana telah meningkatkan kadar penjanaan haba isipadu dan fluks haba permukaan bagi komponennya. Oleh itu, adalah perlu untuk membina suatu teknologi penyejukan yang baru bagi memperbaiki prestasi komponen mikroelektronik, yang mana telah memotivasikan pengunaan jenis struktur gandar dua salutan piezoelektrik sebagai sebuah fan kecil. Struktur dua salutan piezoelektrik ini telah dikaji sebagai makanisma penyejukan alternatif bagi penyejukan komponen mikroelektronik. Parameter seperti panjang, tebal, lebar dan kedudukan bagi lapisan piezoseramik dilakukan pada tahap maksimum telah dikaji dalam kajian ini. Proses ini melibatkan penyelesaian simulasi statik, modal dan harmonik secara berulang. Bagi memahami kelakuan mekanik untuk struktur salutan, analisa static, modal dan harmonic telah dijalankan dengan ANSYS. Bagi produk frekuansi resonan ultrasonic yang pertama dengan melibatkan hujung pesongan dinamik telah digunakan bagi menghasilkan merit prestasi (PM). Untuk mencapai kesan penyejukan maksimum, merit prestasi telah dikaji dan dioptimumkan dengan kaedah neuro-genetik (ANN-GA) berintegrasi telah digunakan bagi mengoptimumkan struktur dua salutan resonan piezoelektrik. Analisa pemindahan haba konjugat 3D telah dijalankan bagi memahami kecekapan dan kebolehpercayaan litar berintegrasi di dalam sistem mikro elektronik.

Teknik pemerhatian aliran (PIV) digunakan bagi mengkaji fungsi kipas piezoelektrik. Kajian ini mendapati pesongan bagi dua salutan member kesan yang ketara pada kelakuan suhu bagi pemalar terikan piezolektrik. Medan elektrik yang digunakan memberi kesan kapada hujung pesongan. Kajian juga mendapati bahawa kipas ini lebih berkesan bagi cip yang mengeluarkan kuasa kurang daripada 0.5W. Teknik PIV juga digunakan bagi meramalkan kedudukan terbaik kipas piezoelektrik bagi memberikan penyejukan lebih baik pada h/lp= 0.16 bagi kedudukan menegak daripada cip yang panas. . Kemudian 2 dimensi simulasi CFD dijalankan dan mendapati persamaan keputusan yang baik dengan data eksperimen dengan perbezaan 11%.

NUMERICAL AND EXPERIMENTAL ANALYSES OF PIEZOELECTRIC FANS FOR MICROELECTRONIC COOLING

ABSTRACT

With the advancement of science and technology, electronic products work faster and perform more functions. Also electronic products are shrinking in size and weight that have increased volumetric heat generation rates and surface heat fluxes over their components. Hence, it is important to develop a new cooling technology to improve performance of microelectronic components, which motivates the usage of cantilever type piezoelectric bimorph structure as a miniature fan. These piezoelectric bimorph structures have been investigated as alternative cooling mechanism for cooling microelectronic components. Parameters such as length, thickness, width and location of the piezoceramic layer to perform at the optimum level are studied here in. This process involves solving static, modal and harmonic simulations repeatedly. To understand the mechanical behavior of the bimorph structure, its static, modal and harmonic analysis are performed using ANSYS. The product of first ultrasonic resonance frequency with the corresponding dynamic tip-deflection has been used to represent the performance merit (PM). In order to achieve maximum cooling effect, performance merit has been studied and optimized with an integrated neuro-genetic approach (ANN-GA) has been applied to optimize the piezoelectric resonating bimorph structure. The 3D conjugate heat

transfer analyses have been performed out using CFD software FLUENT to understand the efficiency and reliability of the integrated circuits in the micro electronic systems. The flow visualization technique (PIV) is used to asses the function of the piezoelectric fan. It is found that the deflection of the bimorph greatly influences the temperature behavior of the piezoelectric strain coefficient. The applied electric field only affect on tip-deflection. It is also found that these fans are more effective for chips dissipating less than 0.5W power. The PIV technique used has predicted the best position of the piezoelectric fan to provide the better cooling at the h/lp=0.16 vertical distance from the heated chip. Latter 2 dimentional CFD simulations were performed and found to be in good agreement with experimental data about 11% variations.

ANALISA BERANGKA DAN EKSPERIMEN KIPAS PIEZOELEKTRIK BAGI PENYEJUKAN MIKROELEKTRONIK

ABSTRAK

Dalam kemajuan sains dan teknologi, produk elektronik bergerak maju dan menjalankan banyak fungsi. Produk elektronik juga telah mengecil saiz dan berat yang mana telah meningkatkan kadar penjanaan haba isipadu dan fluks haba permukaan bagi komponennya. Oleh itu, adalah perlu untuk membina suatu teknologi penyejukan yang baru bagi memperbaiki prestasi komponen mikroelektronik , yang mana telah memotivasikan pengunaan jenis struktur gandar dua salutan piezoelektrik sebagai sebuah fan kecil. Struktur dua salutan piezoelektrik ini telah dikaji sebagai makanisma penyejukan alternatif bagi penyejukan komponen mikroelektronik. Parameter seperti panjang, tebal, lebar dan kedudukan bagi lapisan piezoseramik dilakukan pada tahap maksimum telah dikaji dalam kajian ini. Proses ini melibatkan penyelesaian simulasi statik, modal dan harmonik secara berulang. Bagi memahami kelakuan mekanik untuk struktur salutan, analisa static, modal dan harmonic telah dijalankan dengan ANSYS. Bagi produk frekuansi resonan ultrasonic yang pertama dengan melibatkan hujung pesongan dinamik telah digunakan bagi menghasilkan merit prestasi (PM). Untuk mencapai kesan penyejukan maksimum, merit prestasi telah dikaji dan dioptimumkan dengan kaedah neuro-genetik (ANN-GA) berintegrasi telah digunakan bagi mengoptimumkan struktur dua salutan resonan piezoelektrik. Analisa pemindahan haba konjugat 3D telah dijalankan bagi memahami kecekapan dan kebolehpercayaan litar berintegrasi di dalam sistem mikro elektronik.

Teknik pemerhatian aliran (PIV) digunakan bagi mengkaji fungsi kipas piezoelektrik. Kajian ini mendapati pesongan bagi dua salutan member kesan yang ketara pada kelakuan suhu bagi

pemalar terikan piezolektrik. Medan elektrik yang digunakan memberi kesan kapada hujung pesongan. Kajian juga mendapati bahawa kipas ini lebih berkesan bagi cip yang mengeluarkan kuasa kurang daripada 0.5W. Teknik PIV juga digunakan bagi meramalkan kedudukan terbaik kipas piezoelektrik bagi memberikan penyejukan lebih baik pada h/lp= 0.16 bagi kedudukan menegak daripada cip yang panas. Kemudian 2 dimensi simulasi CFD dijalankan dan mendapati persamaan keputusan yang baik dengan data eksperimen dengan perbezaan 11%.

CHAPTER 1

INTRODUCTION

1.1 Thermal management of electronic systems

1.1.1 Background

Thermal management of electronic components has become major concern for rapid developing electronic industry, specifically in electronic miniaturization process. The miniaturization of electronic systems and increasing demands of minuscule electronic instruments have resulted in substantial increase of volumetric heat generation rates and surface heat fluxes in microelectronic products. The prevalence of high temperature in the electronic equipments may cause deteriorated performance and in some cases result in the failure of the components itself. The thermal management has become more and more important as the demand for compact electronic instruments and miniaturized electronic systems has increased. The augmentation of increased volumetric heat generation rates and high surface heat fluxes are considered to be the major obstacles for optimum and reliable operation of modern high- speed computers and microelectronic systems. The generated heat during the operation of the electronic components should be removed adequately by suitable cooling mechanisms. In recent years, increasing demand of the product compactness, enhancement of the process speeds and the modifications to suit the customer demands have created more

unfavorable performance conditions for these micro electronic systems. Further more, the cost reduction and increased reliability demand by the consumer world have added more complications to the desired performance of the microelectronic systems.

Almost all electronic components either small or big generate heat, this in turn affects the optimum and reliable performance output of the electronic systems if it exceeds the designed maximum sustainable temperature. To avoid the failure and unstable performance of electronic components, the volumetric heat generation rates and surface heat fluxes should be minimized. Due to the rapid development in the miniaturization of the electronic components, the design of the electronic devices has become more compact and hence complex. The reduction in size and increased design complexity has posed various challenges for the task of thermal management of micro electronic systems.

The most common form of fan/heat sink combination for electronic equipments, cooling was employed in the early stages which works on the convection heat transfer principle. But the down sizing of the electronic equipments has resulted in to the increased heat generation and less cooling space, therefore the cooling mechanism with high performance and compact in size is desired.

The National Electronic Technology Roadmap, 1997 has affirmed the expectation that the Moore' law improvements in the semiconductor technology will continue into the second decade of the 21st century which will result in increased heat

load on the integrated chip. In recent years, integrated chips ICs that contain as many as one hundred million transistors embedded on a single chip. This number seems to increase with Moore's Law in future,which increases substantial heat generation in the electronic components. The minimal surface area and increased surface heat flux are the matters of concern to obtain the desirable performance of the IC.

The international technology roadmap for semiconductor 2003, predicts that the junction-ambient thermal resistance should be reduced as low as 0.18ºC/W by the year 2010. Moreover, a survey by the U.S. Air Force indicates that more than 50% of all electronic failures are caused due to the uncontrolled temperature, as evident in Figure 1.1 Yeh and Chu (2002).

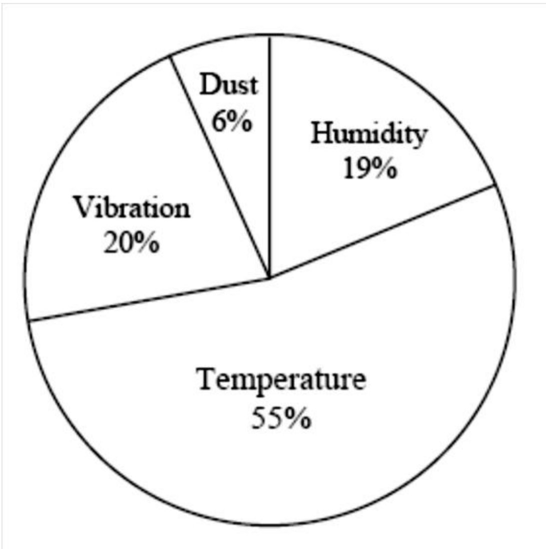

Fig. 1.1 Major causes of electronic failures [Ref:Yeh and Chu, 2002]

Till today various methods have been proposed to counter over heating of the electronic components. The following section describes some of the well known

techniques employed in order to anticipate the various issues in this thermal management area.

1.1.2 Natural Cooling

Convection is defined as diffusion of energy due to random molecular motion as well as energy transfer due to bulk motion. Natural convection occurs where flow is induced by buoyancy forces due to density differences within a fluid. Even though natural convection has a big advantage due to its simplicity, it has one of the lowest heat transfer capabilities (155 – 1550 W/m^2). Generally, this method is of great use for external heat transfer as is found in heat sinks, but not possible for high density internal heat extraction as is needed in hot environment.

1.1.3 Forced Air Cooling

The fluid velocities associated with natural convection currents are naturally low, and thus natural convection cooling is limited to low-power electronic systems. In forced air cooling, the air is made to flow at higher velocities by means of a blower or a fan. In doing, so we can increase the heat transfer rate by a factor of up to about 10, depending on the size of the fan. The normal heat removal capacity of forced air cooling ranges from 800 to 16 000 W/m^2.

1.1.4 Forced Liquid Cooling

Due to higher densities associated with liquids, the use of forced liquid cooling can reach heat transfer rates an order of magnitude greater (11 000 – 930 000 W/ m^2) than when gaseous fluids such as air are used. Some of the disadvantages listed for forced air-cooling are also overcome to some extent. The schematic representation of a forced liquid convection cooling system is shown in Figure 1.2. A coolant liquid is circulated through a flow circuit consisting of a light duty electric pump, a heat exchanger extracting heat from the heated device, a heat exchanger expelling heat to the surroundings, a liquid reservoir and a filter Jiang et al., (2001).

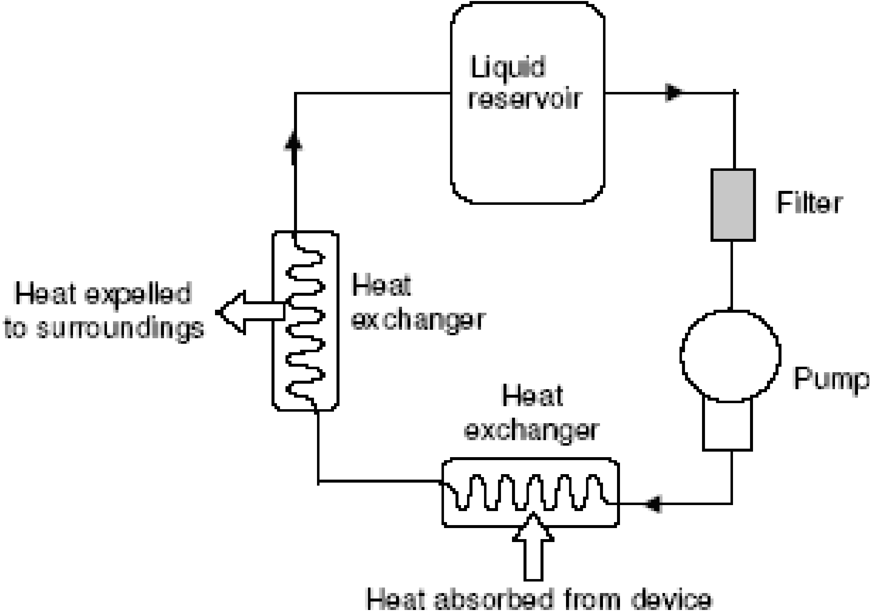

Fig. 1.2. Schematic diagram of a forced liquid convection cooling system

[Ref. Jiang et al., 2001]

1.1.5 Micro-channel heat exchanger

In general, micro-channel refers to conduits of fluids that have a smallest design feature having a scale of micron or larger. In practice, this often means rectangular channels with cross-sectional dimensions of the order of tens or hundreds of microns. Compared with conventional heat exchangers, the main advantage of micro heat exchangers is its extremely high heat transfer area per unit volume. As a result, the overall heat transfer coefficient per unit volume can be as great as $100 MW/m^3K$ which is much higher than conventional heat exchangers Tuckerman and Pease, (1981). The concept of micro-channel heat sinks was first introduced in 1981 by Tuckerman and Pease Hegde et al., (2004) who demonstrated that a heat flux of 790 W/cm^2 can be continuously dissipated while maintaining a temperature difference in the region of 70°C. Figure 1.3 schematically represents a micro-channel heat exchanger. It consists of channels machined or cut into a structure which needs some cooling and a plate covering to enclose a fluid, which is forced through the channels to transport heat to a region where it is expelled to the surroundings Cengel (2004).

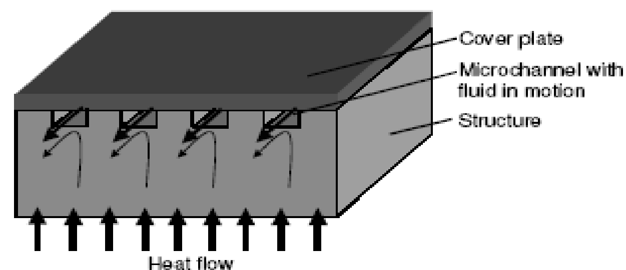

Fig. 1.3 Schematic representation of a micro channel heat exchanger

[Ref: Cengel 2004]

With refrigeration equipment, it is possible to cool a region or component to below the temperature of its surroundings. Heat no longer flows from the component to the surroundings, but is rather pumped by the refrigeration system from the cold component to the hotter surroundings (Federov and Viskanta, 2000). A drawback of this method is the added volume needed to house the liquid circuit, which includes the pump and reservoir.

1.1.6 Heat Conduction via Embedded Solids

Another option is conduction heat transfer through solids laid down within the layered structure of micro-channel. In this way, a thermal path towards heat sinks or other devices is formed and the heat is expelled to the surroundings.. It is easy to manufacture, and has relatively smaller volume and such a system can be accommodated within a micro-channel. This approach may emerge as a possible solution to the thermal problem experienced in micro-channels.

1.1.7 Miniaturized vapor absorption refrigeration

Recently the concept of miniaturized absorption refrigeration system has been proposed for mico electronic cooling. Fig. 1.5 shows schematic diagram of an absorption based heat pump system, which mainly consists of an evaporator, an absorber, a desorber, a condenser, a liquid pump and expansion devices. The working

fluid is water/LiBr pair, where water and LiBr are used as refrigerant and absorbent, respectively.

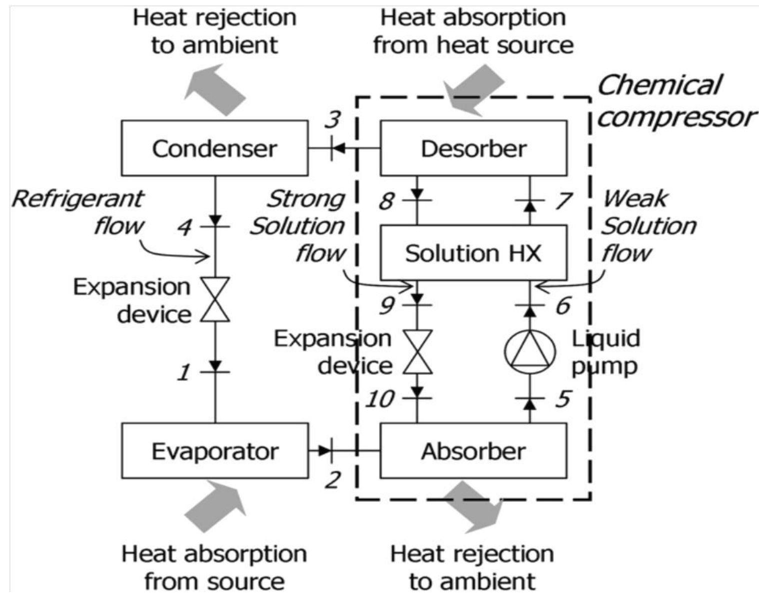

Fig. 1.4 Schematic diagram of an absorption based heat pump system

[Ref: Li Yong and Ruzhu Z. Wang]

The concept of application of the micro-channel refrigeration is the same as that of a walkman/discman. The entire heat pump system can be fitted into a 150mm × 150mm × 100 mm size envelope.

1.1.8 Use of heat pipes as heat sinks

Another way of cooling of electronic devices is the use of heat pipes as the heat sinks. The heat pipes acts as a narrow conduit, which will transmit the heat from the chip to a location where a larger heat sink can be installed.

1.1.9 Impingement or spray cooling

In impingement cooling, different types of nozzles such as orifices or slots, singly or in arrays are used for the cooling purpose of the package. Figure 1.6 shows various configurations of round and slot jets, single and in arrays.

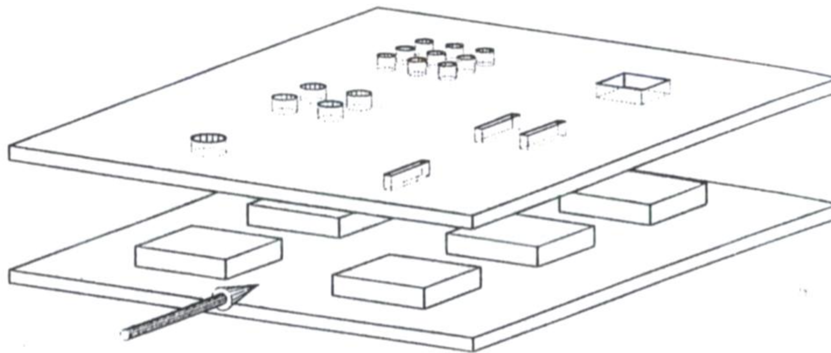

Fig. 1.5 Various configurations of round and slot jets, single and in arrays

[Ref: www.electronics-cooling.com]

1.1.10 Hybrid air-water cooling

The hybrid air- water cooling scheme has been introduced to overcome unusual rise in temperature of the cooling air. With the dramatic increase in power density, use of serial air flow alone would result in a substantial rise in temperature of the coolant. This situation necessitated some means of controlling the temperature of the cooling air as it passed through the system and the hybrid scheme was found to tackle this issue

(Chu and Simons, 1990). With this scheme, heat continues to be removed from the modules of cards by the flowing air. The hot air, however, passes through the air-liquid heat exchanger before arriving at the next board. Analysis of chip junction temperatures in an electronics frame demonstrated reductions in the maximum junction temperature, mean junction temperature, and the range of junction temperatures with the hybrid scheme Antonetti et al., (1973).

1.2 Piezo-Electric Fan for Micro-Electronic Cooling

1.2.1 Introduction

Cooling of low power devices in portable consumer electronics has reached a point where dependence on passive cooling is no longer adequate for keeping the temperatures within prescribed limits. This calls for innovative active cooling solutions. Piezoelectric fans have recently emerged as a viable cooling technology for the thermal management of electronic devices, owing to their low power consumption, minimal noise emission, and small and configurable dimensions. They utilize piezo ceramic patches bonded onto thin, low frequency, and flexible blades to drive the fan at its resonance frequency. The resonating low frequency blade creates a streaming airflow directed at electronic components out of still air (Fig. 1.6). This feature thus obviates the need for input piping or complex fluidic packaging and makes piezo fans ideally suited for the low-profile geometries of portables.

1.2.2 Piezoelectricity and its evolution

Piezoelectricity is a coupling between a material's mechanical and electrical properties. When a piezoelectric material is squeezed, an electric charge collects on its surface. Conversely, when a piezoelectric material is subjected to an electric field, it exhibits a mechanical deformation. A basic illustration of converse piezoelectricity is shown in figure 1.7. Applying an electric voltage to the electrodes of piezoelectric material will induce a mechanical deformation according to the magnitude and sign of applied voltage.

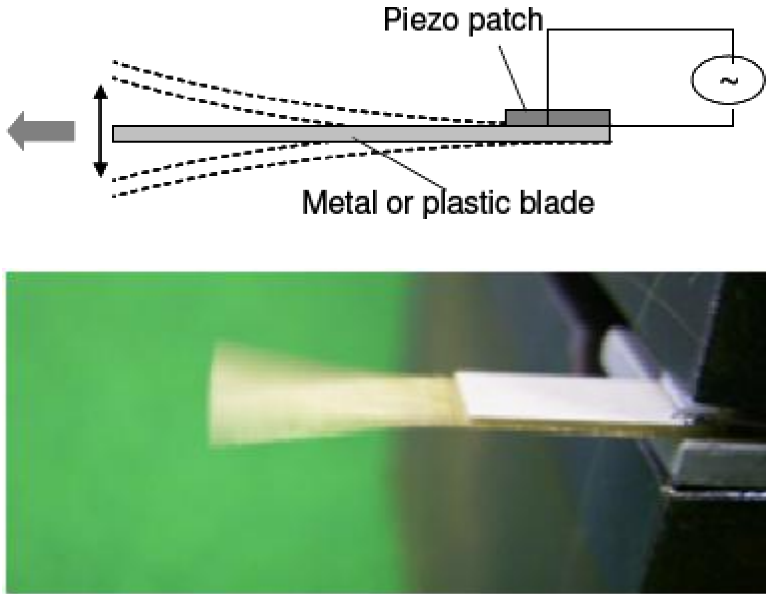

Fig 1.6 Schematic and picture of a piezo fan.

(Source: http://www.electronics-cooling.com)

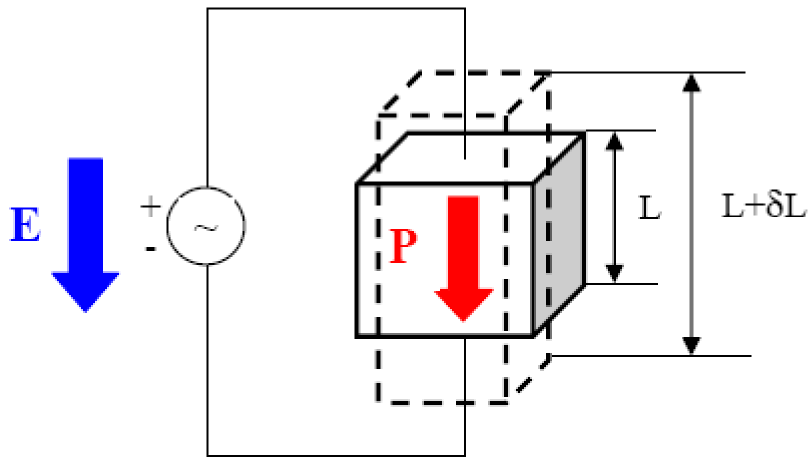

Fig. 1.7 Piezoelectric material changes according to the electric field and polarization direction.

Charles Augustin de Coulomb was the first to introduce the theory of production of electric charge by the mechanical manipulation of solid matter. From 1781 to 1806, he submitted important treatises to the French *Acadamie des Sciences* on electricity and magnetism Gilmour (1971). In 1817 and 1830, René-Just Haüy and Antoine- César Becquerel independently observed that certain crystals showed electrical effects when compressed Graff (1981). However the phenomenon of piezoelectricity was actually discovered in 1880 by Pierre and Jacques Curie, Curie and Curie (1880). While studying the relationships between pyroelectric phenomenon and crystal symmetry, the Curie brothers were able to predict the classes of crystals and the conditions under which electric charge would be observed when the crystals were pressed.

In 1881, Hermann Hankel suggested the term “piezoelectricity” to describe the observed phenomenon. In the same year Gabriel Lipmann predicted the existence of the inverse effect i.e., application of electric charge to opposite crystal surfaces induces deformation. This was confirmed experimentally by Curie brothers in 1882. In 1890, Franz Ernst Neumann formulated the basic principles that govern the behavior of crystals (Nye, 1985). In 1893, Kelvin proposed analogy models and made some basic framework on the modern theory of piezoelectricity Trainer (2003). As an important breakthrough in the 19th century, Voigt developed the tensor equations describing the linear behavior of piezoelectric crystals in 1894.

Voigt published his ‘Lehrbuch der Kristallphysik’, in 1910 and the formulation on piezoelectricity provided in this book has been the source of reference until the mid-20th century.

During the 1920s, Max Born produced theoretical crystal lattice calculations for the piezoelectric coefficient. From 1936, he continued his work on the dynamic theory of crystal lattices Born (1954). Other 20th century pioneers include Walter Cady who in 1921 invented the quartz crystal-controlled oscillator and the narrow-band quartz crystal filter used in communication systems Mason (1975) and Warren Mason who produced further crystal cuts for accurate frequency standards in 1940 Mason (1948) and developed equivalent circuit models for piezoelectric resonator.

By the early 1950s barium titanate ($BaTiO_3$) ceramic was established as a piezoelectric transducer material Berlincourt (1981). In 1954, lead zirconate titanate or PZT ceramics were developed and replaced barium titanate in all fields of piezoelectric applications and they are the most widely used owing to their excellent properties. Due to their permanent electrical and mechanical asymmetry, the unit cells of PZT exhibit spontaneous polarization and deformation. Because of the random distribution of the cell orientation in the ceramic materials, a ferroelectric poling process is required to obtain the piezoelectric properties. However, if heated above the Curie temperature, the PZT crystallite unit cells take on isotropic structure. When cooled, the material does not regain its macroscopic piezoelectric properties. Further developments from 1960s to the current stage will be discussed in Chapter 2.

1.2.3 Piezoelectric Materials

As the piezoelectric effect is transfer between electrical and mechanical energy, it can occur only if the material is composed of charged particles and can be polarized. For a material to exhibit an anisotropic property such as piezoelectricity, its crystal structure must have no centre of symmetry. Most of the piezoelectric materials are crystalline solids. They can be single crystals, either formed naturally or by synthetic processes, or polycrystalline materials like ferroelectric ceramics. Certain polymers can also be made piezoelectric by stretching under an electrical field. Most commonly available materials are Piezoelectric Ceramics (PZT) and Piezoelectric Polymers (PVDF).

PZT is formed by conventional ceramic processing techniques, such as dry pressing, casting or extrusion. The ceramic material is then sintered, machined into the desired dimensions and pasted on electrodes. Polarization of the ceramic element is the final step in processing which involves heating the ceramic above the Curie temperature and subsequently cooling the material in the presence of a strong DC electric field. This poling process aligns the molecular dipoles of the ceramic in the direction of the applied field and thus induces its piezoelectric properties.

PZT is extremely stiff, hard, chemically inert and completely insensitive to humidity or other atmospheric influences. It is capable of exerting or sustaining greater stresses. Moreover the properties of PZT can be optimized to suit specific applications by appropriate adjustment of the zirconate-titanate ratio.

The PVDF (Polyvinylidene Fluoride) can be made piezoelectric as fluorine is much more electronegative than carbon. The fluorine atoms will attract electrons from the carbon atoms to which they are attached. A sequence of processes, including elongation, annealing, evaporation of electrodes and poling, have to be performed to make the material piezoelectric. The maximum operating temperature of PVDF (90^0C) is much lower than that of PZT (140^0C) which makes it less useful working in high temperature environment. The advantage of PVDF over PZT is that the maximum electric field strength that can be applied to the polymer without danger of depolarization is much greater.

1.2.4 Piezoelectric Actuators

Piezo electric actuator is a device which transforms energy into controllable motion. The basic characteristics of any linear actuator are displacement, force, frequency, size, weight and electrical input power. Piezoelectric materials are known for their excellent operating bandwidth and can generate large forces in a compact size, but they have very small displacements. Hence some sort of amplification is required before they could be put into use.

For the piezoelectric actuators, the researchers focused on developing means to amplify the deflection of the material. Piezoelectric actuation architectures can generally be placed into one of three categories based on the amplification scheme Niezrechi et al., (2001): externally leveraged, internally leveraged and frequency leveraged. Externally leveraged actuators including Moonies rely on an external mechanical component for their actuating ability. Internally leveraged actuators generate amplified strokes through the internal structure without the use of an external mechanical component. These include stack, bender, rainbow, thunder etc. Frequency leveraged actuators rely on an alternating control signal to generate motion. A few examples of amplification schemes are given as below:

1.2.4.1 Stacks: A large number of piezo layers can be stacked to linearly increase their overall deflection while maintaining a low voltage requirement, as shown in figure 1.8. The displacement and force of a stack actuator are directly proportional to the

actuator length and cross-sectional area, respectively. Stacks have been widely used independently or as an input to extremely amplified schemes. The piezoceramic stacks show applications in the vibration control Remond and Barney (1997), suspension control Fukami et al., (1994) and vibration damping in machine tools Martinez et al., (1996).

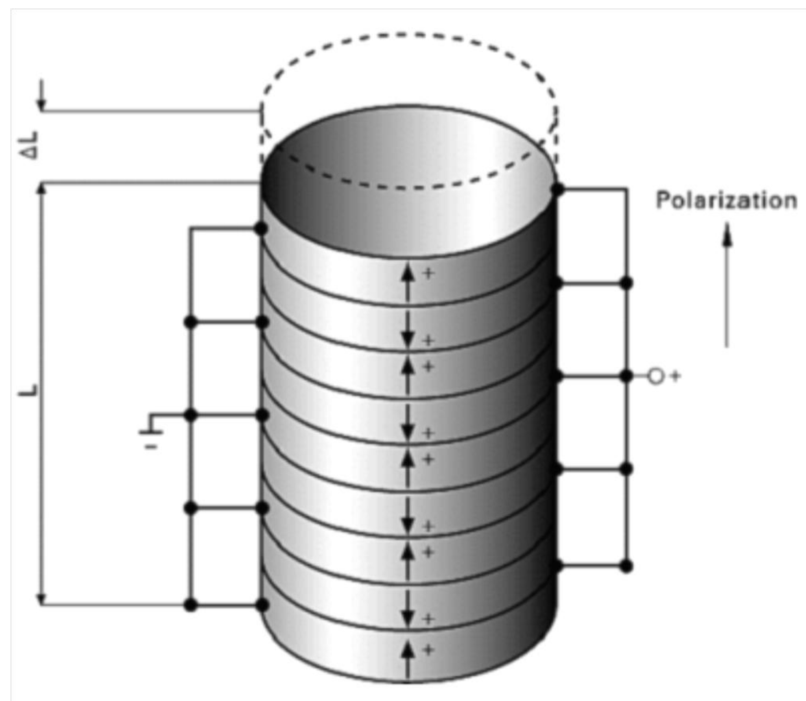

Fig. 1.8 Diagram of piezoelectric stack

(Source: http://www.physikinstrumente.com/tutorial)

1.2.4.2 Unimorph: A unimorph is a composite beam, plate or disk with one active layer and one inactive layer, or substrate. rainbow and thunder actuators are typically

referred to as unimorph actuators. rainbow or Reduced and Internally Biased Oxide Wafers are piezoelectric wafers with an additional heat treatment step to increase their mechanical displacements. In the rainbow process, developed by Gene Heartling at Clemson University, typical PZT wafers are lapped, placed on a graphite block, and heated in a furnace at 975 C for 1 hour Furman et al., (1994). The heating process causes one side of the wafer to become chemically reduced. This reduced layer, approximately 1/3 of the wafer thickness, causes the wafer to have internal strains by which the flat wafer is shaped into a dome. The internal strains cause the material to have higher displacements and higher mechanical strength than a typical PZT wafer. RAINBOWs with 3 mm of displacements and 10 kg point loads have been reported Haertling (1990). A rainbow stack actuator is shown in figure 1.9.

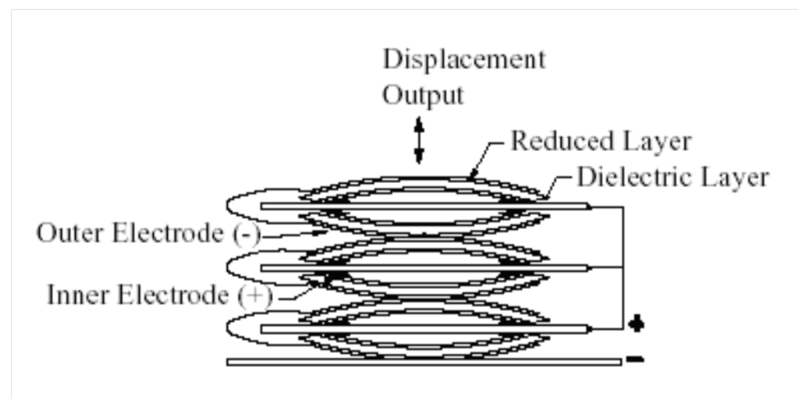

Fig. 1.9 A rainbow stack actuator

(Source: http://www.physikinstrumente.com/tutorial)

Another actuator that uses a prestressed configuration is the thunder actuator. thunder was developed at the NASA Langley Research Center in 1994. The actuator

consists of a layer of a ceramic wafer attached to a metal backing using a polymide adhesive film as in shown in figure 1.10. The manufacturing process is performed using a high temperature and high pressure environment resulting in an actuator that can withstand high levels of mechanical and electrical loading Bryant (1996); Mossi et al., (1998); Mossi et al., (1999). Comparing rainbow actuator with thunder, it is shown that rainbow generates 10% to 25% more displacement than comparable thunder actuators Wise (1998) Kugel et al., (1997). The significant advantage of thunder actuators is their extremely rugged construction which allows them to be more readily used in commercial applications.

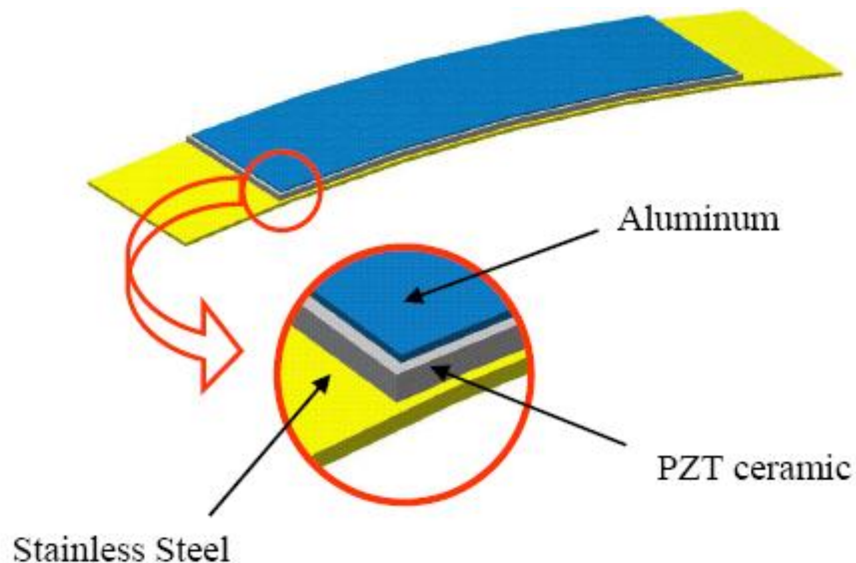

Fig.1.10 Layers in a thunder actuator

(Source: http://kasml.konkuk.ac.kr/data/Fully%20coupled.ppt)

1.2.4.3 Bimorph: Piezoelectric bimorph is a bending element that generates horizontal displacement at the drive of electric field using the converse piezoelectric effect. Bimorph actuator usually consists of two thin ceramic plates bonded together and driven with opposite electric field. One plate expands while the other contracts. The net result is a lateral deflection of the plates. There are two different electrical connections which are usually used in bimorph fabrication: one is series connection in which two piezoelectric plates have opposite polarization directions and the actuator is driven by applying electrical field between the top and bottom electrodes (see figure 1.11(a)); the other is parallel connection in which two piezoelectric plates are of the same polarization directions and the actuator is driven by applying electrical field between surface electrodes and the bonding layer (see figure 1.11(b)). In the latter case, two ceramic plates are electrically connected in parallel and driven voltage is applied across half the actuator thickness, thus enabling half driving voltage to achieve the same electrical field as in the series case. Usually a metallic sheet or middle shim is sandwiched between the two piezoelectric plates to increase the reliability and mechanical strength. Unlike the PZT stack, bimorphs are operated in the 31 d mode.

Bimorphs were first developed in the early 1930s by Sawyer at the Brush Development Company. However, the performance of these actuators was understood at a rudimentary level until much later, when research into smart structures became more detailed Steel et al., (1978); Tzou (1989). Bimorphs have been used in robotic applications for which large displacements are desired Chonan et al., (1996), spoilers on

missile fins August and Joshi (1996) and actuation for a quick-focusing lens Kaneko et al., (1998).

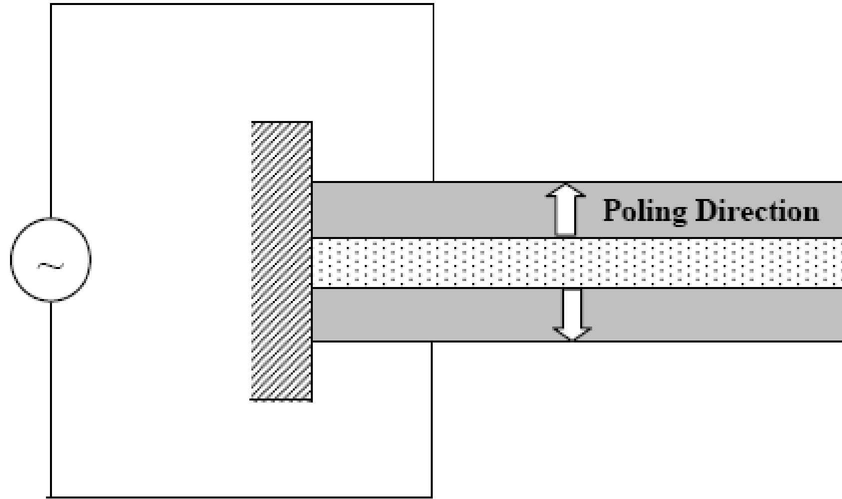

(a) Bimorph in series connection

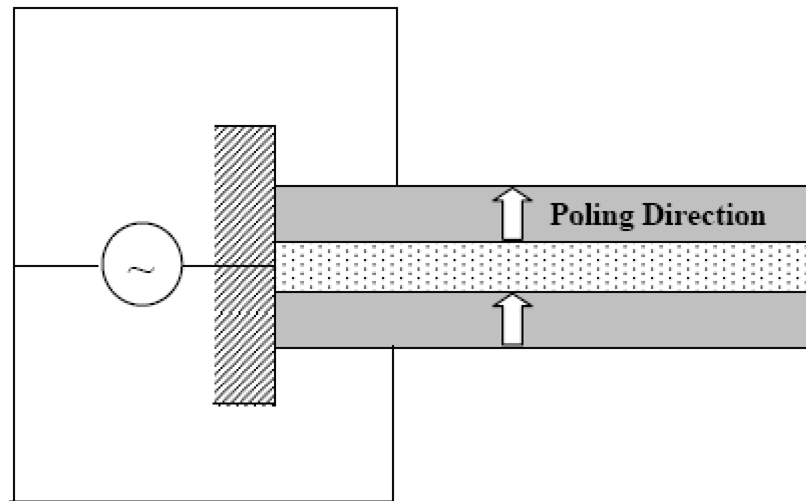

(b) Bimorph in parallel connection

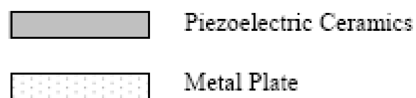

Fig. 1.11 Structure of cantilever bimorph

Plentiful research works have been carried out experimental as well as numerical simulation by using flexural waves. The application of piezoelectric materials in sensors and actuators for actuating and controlling the smart structures were extensively studied by Luis and Crawly. The potential convective heat transfer capability of an UFW generated by direct and inverse piezoelectric effect was experimentally investigated by Ro and Loh.

There are several parameters like length, thickness and location of the piezoceramic layer to perform at the optimum level. The product of first ultrasonic resonance frequency with the corresponding dynamic tip-deflection has been used to represent the performance merit (PM). Recent developments in miniaturization of electronic components necessitate the optimal design of the resonator structures to generate the maximum cooling effect. To achieve maximum cooling effect, one has to maximize performance merit. This process involves solving static, modal and harmonic simulations repeatedly. These analyses are complicated which takes substantial amount of computer resources and require sound knowledge of working with ANSYS. Further more the applications of artificial neural network (ANN) and genetic algorithm (GA) approaches in optimization of piezoelectric resonating bimorph structure has been noticed in the recent articles. ANN has been widely accepted as notable solution for modeling complex non-linear systems if the historical data is available. In recent years, ANN has been successfully applied in various fields such as control, finance, aerospace, electronics, industrial and manufacturing. Philipp Burmann et al. have studied optimization of piezoelectric fans by using analytical Bernoulli-Euler model and finite

element model of the composite beam. They maximized electromechanical coupling factor for their optimization studies. Tolga Acikalin et al. performed experimental investigation of thermal performance of piezoelectric fans. They build prototypes of fans and observed their feasibility as a cooling device and obtained their optimal locations. In similar way many researchers studied the various aspects of the piezoelectric fan performance, its design optimization and the numerical and experimental study of the conjugate heat transfer phenomenon of the chip to evaluate the influence of the piezofan as well which has been discussed in detail in the subsequent chapter.

1.3 Problem Statement

The increasing demand of portable electronic devices such as cell phones, laptops have become inevitable in our daily life and information processing.Increased popularity and consumer demand has resulted in more powerful electronic components to be crammed into smaller and smaller spaces as in a typical microprocessor as shown in figure 1.12. This makes the electronic products to be more powerful, reliable, lighter, smaller, less expensive and at the same time to be faster, user-friendly with additional functional features. To attain these abilities, technologies have been developed from small-scale integration (SSI) to very large-scale integration (VLSI) and thereafter more advanced ultra-large-scale integration (ULSI) going towards ever-larger-scale circuit integration on a single chip. Due to the functional and performance requirements of modern and future electronics, the technology experts in the semiconductor industry

envision the era of gigascale integration (GSI) and terascale integration (TSI), where many billions and trillions of transistors may be integrated on a single semiconductor chip. This integration follows the very well known "Moore's law" (figure 1.13). As per Moor's law. the number of transistors used in an integrated circuit doubles in every 18 months. In fact, present Pentium-IV computer processor consists of more than 42 million transistors in a single chip, which is almost equal to the size of a postage stamp.

The miniaturization of electronic products increases volumetric heat generation rates and surface heat fluxes over its components. This excess heat reduces the performance of chips and can ultimately destroy the delicate circuits. Hence there is a greater need for effective cooling strategies to ensure proper performance. In the present scenario, cooling by conventional means include the use of rotational fans for active cooling and heat sinks for passive cooling. Active cooling techniques are not suitable due to the limited space, noise restrictions, high power consumption and many more. The cramped interiors of microelectronic devices contain empty spaces that are too small to house conventional fans. With increase in the complexity of microelectronic systems, directing airflow to each component of the system becomes more constrained. Miniaturization of these devices limits the usage of larger heat sinks. This was anticipated by researchers who came with new idea of piezoelectric fans technique for the miniaturized devices cooling. Piezoelectric fans are considered as promising substitute to augment convection currents where space, power and noise are of primary concern. Many researchers have contributed in this filed by their remarkable findings in the piezoelectric fans cooling. But there is a need to address many issues in

this area which are to be explored to get the piezoelectric fan cooling efficient and effective. The present study emphasizes on the design, optimization and performance analysis of a piezoelectric bimorph actuator.

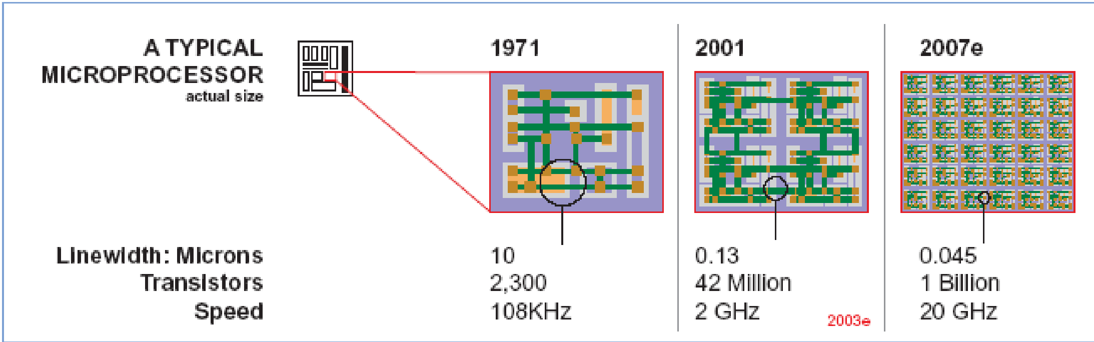

Fig. 1.12 Chronological Variation in chip density of microprocessor

[Ref: www.electronics-cooling.com]

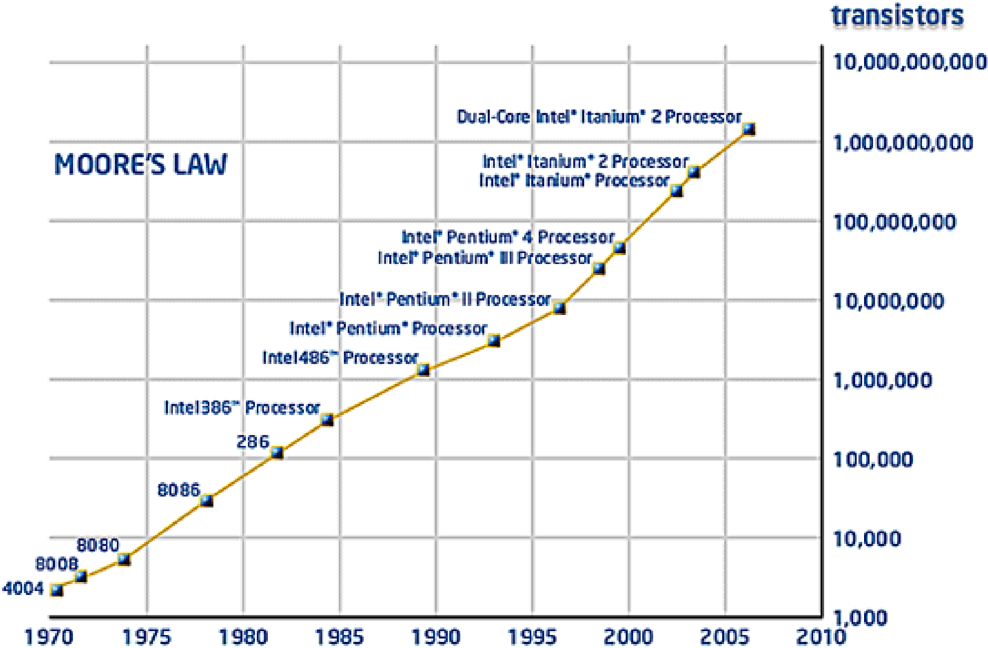

Fig. 1.13 Moore's law showing the increase in circuit complexity over time